Original Article
Food Science and Technology
ISSN 0101-2061 (Print)
ISSN 1678-457X (Online)
DOI: https://doi.org/10.5327/fst.561
CC BY

Ecological films based on natural polymers incorporated with Amazonian fruit flour

Ana da Silva Torres VIANA[1*], Atos Henrique SANTOS[1], Juliana Aparecida CÉLIA[1], Maria Siqueira de LIMA[1], Kênia Borges de OLIVEIRA[1], Marco Antônio Pereira da SILVA[2], Geovana Rocha PLÁCIDO[2]

Abstract

Biodegradable films were produced using a blend of carboxymethyl cellulose, orange pectin, zinc nanoparticles, and rice wax, incorporating balanced ingredients from Amazonian fruits, *Couepia bracteosa* Benth and *Pouteria caimito*. The films were produced by the casting technique and characterized for their physical, optical, mechanical, thermal, water vapor permeability, infrared spectroscopy, and biodegradability properties. Films composed of fruit flours were thicker than the control, and those compounded with rice wax showed high solubility and low vapor permeability. The mechanical properties of the control film and those compounded with pajurá flour showed the best results. Fourier-transform infrared spectroscopy showed that the functional groups of pectin and carboxymethyl cellulose are similar, resulting in peak overlap. Films with higher flour concentrations were darker. Biodegradability occurred within approximately 15 days. Films made of carboxymethyl cellulose, pectin, zinc nanoparticles, and 40 and 50% pajurá flour stood out as excellent edible films with remarkable properties of permeability, mechanical resistance, and thermal stability. These films have the potential for application in various foods, especially those requiring protection against moisture and light.

Keywords: biodegradable films ; *Couepia bracteosa*; *Pouteria caimito*.

Practical Application: Eco-films developed from natural polymers and Amazonian fruit flour can be applied as sustainable alternatives to conventional plastic packaging. These films enhance biodegradability, add functional properties from the fruit bioactive compounds, and may be used in food preservation, contributing to environmentally friendly packaging solutions.

1 INTRODUCTION

Amazonian fruits stand out and are increasingly attracting the interest of consumers and researchers due to their sensory, nutritional, and bioactive potential. Many of them can be explored as food and therapeutic plants, especially as antioxidants and antimicrobial agents, contributing to the sustainable development of the Amazon region (Araújo et al., 2021).

The characteristics of some species, such as *Couepia bracteosa* (pajurá) and *Pouteria caimito* (abiu), considered promising sources of bioactive compounds, reveal potential applications in the pharmaceutical, cosmetic, and food industries (Abreu, 2018; Berto et al., 2015). In addition to this, the use of biodegradable materials such as macromolecules derived from proteins and carbohydrates has gained prominence in packaging production due to their ecological properties and as substitutes for petroleum-derived polymers (Pirouzifard et al., 2020; Shivangi et al., 2021; Silva et al., 2018).

Carboxymethyl cellulose (CMC) is one of the most common derivatives of cellulose used in the preparation of edible films. CMC is a long-chain linear polysaccharide, soluble in water and anionic; its solution has high viscosity with non-toxic and non-allergenic effects. It is cost-effective, biocompatible, biodegradable, and possesses excellent film-forming properties (Dashipour et al., 2015; Ezati et al., 2022; Kouhi et al., 2020).

Pectin is a versatile biomaterial considered an effective biopolymer for the production of edible films due to its biocompatibility, biodegradability, and non-toxicity. Pectin has the potential to transport functional substances and combine ingredients with distinct characteristics to generate synergistic effects, promising in the creation of new composite films (Gan et al., 2022; Nisar et al., 2018).

The combination of fruit flours or powders stands out in the manufacture of environmentally conscious and renewable products. Derived films exhibit moderate oxygen permeability and acceptable mechanical properties, making them a viable option for edible packaging (Martelli et al., 2013). In this context, flours derived from Amazonian fruits (*Couepia bracteosa* Benth and *Pouteria caimito*) can enrich the nutritional value and improve the sensory aspects of films when incorporated into final products (Andrade, 2014).

Optimization of packaging properties can be achieved by incorporating inorganic elements such as zinc oxide nanoparticles (NPsZnO). NPsZnO can improve mechanical resistance, barrier properties, and stability (Emamhadi et al., 2020; Espitia,

Received: Oct. 02, 2025.
Accepted: Oct. 07, 2025.
[1]*Instituto Federal Goiano, Postgraduate Program in Food Technology, Rio Verde, Goiás, Brazil.*
[2]*Instituto Federal Goiano de Educação, Ciência e Tecnologia, Rio Verde, Goiás, Brazil.*
*Corresponding author: ana.viana@estudante.ifgoiano.edu.br
Conflict of interest: nothing to declare.
Funding: This work was supported by Instituto Federal Goiano (IF Goiano), FINEP (Funding Authority for Studies and Projects), CAPES (Coordination for the Improvement of Higher Education Personnel), and FAPEG (Research Support Foundation of the State of Goiás).

2013). The inclusion of lipid compounds, such as waxes, contributes to improving water vapor barrier properties, although it may result in opacity and limited flexibility (Andrade, 2014). Therefore, the synergy between biopolymers aims to maximize the potential of each component, aiming for more comprehensive and beneficial results.

In this study, the formulation of blends for the production of edible films was investigated, combining CMC, orange pectin, zinc nanoparticles, and rice wax in a harmonious manner with the fruit riches of the Amazon. The core of this research lies in the creation of compositions based on plant resources, integrating suitable mechanical and physicochemical properties, coupled with intrinsic biodegradability, to make them ideal for post-harvest applications in fruits.

1.1 Relevance of the work

The study proposes the development of biodegradable films made from natural polymers and flours of Amazonian fruits, such as *Couepia bracteosa* and *Pouteria caimito*. The research values regional resources, promotes sustainability, and offers an ecological alternative to conventional plastics. The films exhibited good mechanical, thermal, and barrier properties, as well as rapid biodegradability, showing potential for use as edible and sustainable packaging in the food industry. This approach integrates technological innovation and environmental preservation, contributing to the utilization of Amazonian biodiversity and the advancement of high-performance ecological materials.

2 MATERIAL AND METHODS

2.1 Material

Oranges for pectin extraction were obtained from the farm of the Federal Institute of Goiano – IF Goiano, in the municipality of Rio Verde – GO, Brazil (–17.801997, –50.904153) in May 2022. The fruits were in the initial ripening stage, characterized by a yellowish-green color, intact skin, and firm to the touch. The *Couepia bracteosa* (pajurá) fruit was harvested in a community located in the municipality of Candeias do Jamari - RO, Brazil (–8.781456, –63.602387). The *Pouteria caimito* (abiu) fruit was acquired at the regional market located in the Municipality of Porto Velho- RO, Brazil (–8.757711, –63.882143) in May 2022. CMC (as sodium salt) (Sigma-Aldrich). Rice wax (Megh Indústria e Comércio LTDA). Zinc nanoparticles were produced in the laboratory of IF Goiano.

2.2 Pectin extraction

In the Fruit and Vegetable Laboratory of the Federal Institute of Goiano - Rio Verde Campus, oranges (Citrus sinensis) were sanitized in chlorinated water (100 mg.L-1) for 3 min. After being washed in running water, the fruits were peeled with the help of a sharp knife, cut in half, and had their pulp and seeds removed. Subsequently, the albedo was cut into pieces, placed on trays, and subjected to the drying process in an oven at a temperature of 60 °C for 24 h. The dried material was ground in a knife mill until a fine flour was formed, stored in airtight glass jars, and kept refrigerated at 4 °C.

Pectin was extracted from the albedo flour in an acidic medium, according to Munhoz et al. (2010), with modifications. 16 g of orange albedo flour, 33 g of P.A. citric acid (Synth) in 640 mL of distilled water were added. This mixture was kept under constant stirring on a Magnetic Stirrer (SP 162-SP LABOR) and heated until it reached a temperature of 80 °C. After that, the mixture was left for another 1 h under agitation with temperature control. At the end of the specified time, the sample was cooled to a temperature of 4 °C. Then, it was filtered through a 150-micron nylon cloth, and to the obtained filtrate, absolute ethyl alcohol P.A. (LS Chenicals®) was added in a ratio of 1:2. The solution was left to stand for 1 h for pectin precipitation. The coagulated pectin was separated by filtration through nylon cloth and washed with 200mL of 70% ethyl alcohol, followed by washing with 200mL of 95% ethyl alcohol to remove extraction residues. The gel obtained in the filter was then dried in an oven at 60 °C for 24 h until a constant weight was achieved. The dry pectin was ground in a knife mill and stored in airtight glass jars.

The calculation of the pectin yield was done according to Munhoz et al. (2010), based on the initial mass of the orange flour used (Equation 1).

$$\text{Yield (\%)} = \frac{\text{mass of pectin obtained after extraction and drying (g)x100}}{\text{mass of the sample on a dry basis (g)}} \quad (1)$$

2.3 Preparation of Amazonian fruit flour

The transportation of pajurá and abiu fruits to the IFGoiano campus - Rio Verde was carried out by cargo transport, packaged in a refrigerated environment to prevent loss. The fruits were sanitized, peeled, pulped, and dried in an oven at 60 °C until reaching a constant weight. The material was ground in a knife mill and stored in a refrigerator for later use.

2.4 Obtaining zinc nanoparticles

To obtain zinc nanoparticles, the method was based on the reference work of Sathiya et al. (2018) and involved the use of microwave irradiation (Panasonic, 20L, model CMA20BBB-NA/220W). Firstly, a 0.3 M solution was prepared by dissolving dehydrated zinc acetate in distilled water. The pH of the solution was adjusted to 10 by adding 2 M NaOH (GR grade from Merck). The solution was irradiated for 1 h in a domestic microwave, filtered, and washed with distilled water and ethanol until free from impurities. The precipitate was irradiated for 1 h in a microwave oven, and then, the samples were dried at room temperature at 25 ± 2 °C for 72 h.

2.5 Preparation of rice wax emulsion

Rice wax was prepared in the form of aqueous-in-oil (A/O) emulsion with a concentration of 8%, following the methodology used by Rodrigues et al. (2014), with minor adaptations. The wax was heated to a temperature above 85 °C in a beaker with stirring. Simultaneously, an aqueous solution containing Tween 80 (polysorbate 80) and Span 80 (sorbitan monooleate

80) as emulsifiers (at concentrations of 14.4% w/w and 5.6% w/w, respectively, based on the dry weight of the wax) was also heated to 85 °C. Under continuous stirring, this mixture was added to the melted wax. The emulsion was then processed in a 400 W ultrasonic device (UP400S, Hielscher, Teltow, Germany), operating at a frequency of 24 kHz in 10 alternating cycles, with pause intervals of 15 sec between each cycle.

2.6 Preparation of composite films

The production of the films was carried out following the casting technique (López et al., 2011; Turbiani & Kieckbusch, 2011) with modifications.

As detailed in Table 1, each solution was obtained by dissolving CMC and pectin in distilled water and subsequently adding the composites pajurá flour, abiu flour, zinc nanoparticles, and rice wax.

The CMC was dissolved in distilled water (solution A) in a beaker and placed on a hot plate stirrer at 50 °C for complete dissolution until a clear mixture was obtained. Simultaneously, the pectin was dissolved in a separate beaker (solution B) in distilled water, kept under heating and constant stirring for 20–35 min at 70 °C. Solutions A and B were mechanically mixed using a glass rod. To these base solutions, glycerol (30, 40, 50%), NPsZnO (10%), rice wax (15%), pajurá flour (5, 30, 40, 50%), and abiu flour (5, 30, 40, 50%) were added according to each formulation (Table 1). The solutions were homogenized and sonicated (Ultrasonic Washer, Ultronique, Q3.0/40, Brazil) in three cycles of 30 min to remove bubbles from the solution.

The components were added based on the total weight of CMC and pectin, which combined totaled 2g. Thus, the proportions of glycerol, NPsZnO, rice wax, pajurá flour, and abiu flour were calculated on the combined mass of 2g, i.e., (w/w of total solids).

After preparation, the film-forming solutions (100ml) were deposited on acrylic plates with a diameter of 14 cm and dried by dehydration in a conventional oven for 24 h at 40 °C (Jesus, 2017; Silva, Bierhalz, & Kieckbusch, 2009).

Subsequently, the dried films were stored for 72 h in desiccators at a relative humidity of 52% (saturated magnesium nitrate solution) and a temperature of 25 °C to standardize their moisture content for analysis.

The variation in the concentrations of the compounds resulted from experimental adjustments focused on essential properties such as visual appearance, color uniformity, homogeneity, ease of peeling, and handling resistance. We prioritized these characteristics, adjusting the concentrations to meet the practical and technical requirements of the application.

2.7 Characterization of films

2.7.1 Thickness and moisture content

Measurements were taken on three films from each treatment, with each film measured at 10 random points in different segments. The equipment used was the digital micrometer (Mitutoyo, MDC-25PX, Japan) with a capacity of 0–25 mm and a resolution (precision) of 0.001 mm.

Following the AOAC methodology (Association of Official Analytical Chemists International, 2005), film samples for moisture content determination were cut into standardized dimensions of 2cm^2 each and weighed before and after drying. The moisture content was determined by the percentage of mass loss after drying in an oven at 105 °C for 24 h (Equation 2).

$$\text{Moisture (\%)} = \frac{(\text{mi} - \text{mf})}{\text{mf}} \times 100 \quad (2)$$

In which:

Moisture (%) is the percentage of water evaporated from the film;

mi is the initial mass of the film; and

mf is the final mass of the film after drying.

2.7.2 Solubility and water vapor permeability

The determination of solubility was conducted to assess water resistance and film integrity in aqueous systems. Samples in triplicate, with standardized dimensions of 2cm², were dried in an oven at 105 °C for 24 h and weighed to obtain the initial weight. Subsequently, the dried samples were immersed in 50 ml of distilled water, kept under constant and slow agitation at 25 °C for 24 h on a magnetic stirrer (Warmnest, Virginia, USA). After the agitation period, the samples were filtered, and the

Table 1. Detailed concentrations and compositions of film-forming solutions, defined for specific analyses aimed at exploring physical-chemical and mechanical properties.

Solution	CMC/Pec	CMC	Pectin	Rice wax	Pajurá flour	Abiu flour	Glycerol	NPsZnO
	(%)	(g)	(g)	(g)	(g)	(g)	(g)	(g)
CP	50/50	1.0	1.0	0	0	0	0.8	0
CP-P40	50/50	1.0	1.0	0	0.8	0	0.8	0
CPZ-P40	50/50	1.0	1.0	0	0.8	0	0.8	0.2
CPZ-P50	80/20	1.6	0.4	0	1.0	0	0.8	0.2
CP-A40	50/50	1.0	1.0	0	0	0.8	1.0	0
CPZ-A50	80/20	1.6	0.4	0	0	1.0	0.8	0.2
CP-AC	50/50	1.0	1.0	0.3	0	0.1	0.8	0
CPZ-PC	20/80	0.4	1.6	0.3	0.1	0	0.8	0.2

CMC: carboxymethyl cellulose.

remaining material was dried again in an oven at 105 °C for 24 h, allowing the determination of the amount of undissolved dry matter (Chiumarelli & Hubinger, 2012).

The determination of the content of dissolved dry matter after 24 h of immersion in water (Equation 3).

$$MS\ (\%) = \frac{(mi - mf)}{mf} 100 \quad (3)$$

In which:

MS (%) is the percentage of dissolved dry matter;

mi is the mass of the film after the first drying; and

mf is the mass of the film dried after the second drying.

Water vapor permeability (WVP) was measured gravimetrically at 25 ± 2 °C using the ASTM E96/96 M-16 method, with adaptations. Film samples in disk format (8 cm diameter) were sealed in a permeation cell containing silica gel and placed in desiccators with distilled water. The cell was weighed every 1 h for 9 h using an analytical balance. The WVP (polyvinyl alcohol, PVA) of the film was calculated using Equation 4.

$$WVP = \frac{W.X}{T.A.\Delta P} \quad (4)$$

In which:

«x» is the average thickness of the film;

«A» is the permeation area of the film (in m^2); and

«ΔP» is the difference between the partial pressure of the atmosphere over the silica gel and over the pure water (3.168 kPa at 25 °C).

The term «w/t,» where «w» represents the weight gain in the permeation capsules and «t» is the time, was calculated by linear regression based on the weight gain data over time. This method allowed for the determination of the water vapor permeation rate of the film.

2.7.3 Mechanical properties

For the execution of these analyses, a universal testing machine (Instron, model 3367, Grove City) was utilized. Additionally, a Texture Analyzer (TA-XT Plus, England) was employed. The tests were conducted in a controlled environment at 25 ± 1 °C temperature and 55% ± 3% relative humidity. The film samples were cut with a width of 25.0 mm and a length of 120 mm. The average thickness of the films ranged from 0.07 ± 0.04 mm to 0.08 ± 0.02 mm. Prior to the tests, the samples underwent a preconditioning process, remaining in desiccators containing magnesium chloride, with humidity maintained at 55% and temperature at 25 °C, for 48 h.

2.7.4 Fourier transform infrared spectroscopy

The Fourier transform infrared spectra (FTIR) were obtained using an FTIR-ATR-NIRA equipment (Frontier PerkinElmer, Waltham, USA). Each sample underwent 60 scans in the spectral range of 600–4000 cm^{-1}, with a resolution of 4 cm^{-1}.

2.7.5 Thermal stability analysis

The thermal properties of the films were analyzed using a thermogravimetric analyzer (Netzsch, STA 449 F3 Nevio, Germany). Approximately 10 mg of each sample was weighed into open Alumina crucibles (85 µL). The temperature range studied was from 30 to 600 °C, with a heating rate of 10 K/min, under a nitrogen atmosphere (50 mL/min). Changes in mass were continuously recorded as a function of temperature.

2.7.6 Color analysis

The instrumental color parameters were determined using a colorimeter (Chroma Meter CR-400—KONICA MINOLTA, USA), according to the values of brightness L* (variation from light to dark), chromaticity a* (variation in the green to red axis), and chromaticity b* (variation in the blue to yellow axis), as well as saturation parameters (Croma-C*) (Equation 5).

$$C = \sqrt{a*^2 + ba*^2} \quad (5)$$

The movie was divided into four quadrants, and in each sample, four readings were taken in each of these quadrants.

2.7.7 Biodegradability test

The films were placed in containers containing soil with constant moisture, simulating the natural biodegradability process, according to American Society for Testing and Materials (ASTM, 2009) standard.

The soil was prepared by combining sand, soil, and manure. This plant substrate was treated in the Fruit and Vegetable Laboratory of IF Goiano - Rio Verde. The test specimens, with dimensions of 3 cm^2, were identified and placed in 250-mL beakers containing 200g of soil, positioned 3 cm below the soil surface in a Biological Oxygen Demand (BOD) chamber, maintained at a temperature of 30 °C and relative humidity of 99%, ensuring constant soil moisture.

The experiment was conducted in triplicate and evaluated at specific intervals of 72 h. After each designated period, the films were unearthed with the aid of a brush, removing as much soil residue as possible. Subsequently, they were photographed for visual analysis and discussion.

2.8 Statistical analysis

The experiment adopted a completely randomized experimental design, using an 8 x 10 factorial scheme. Each formulation among the eight treatments corresponds to a specific

configuration of factor levels, allowing for a comprehensive evaluation of the individual effects and interactions between factors on the properties of the composite films.

The evaluations in this study were conducted in triplicate to ensure consistency and accuracy of the results. The obtained data were subjected to analysis of variance (ANOVA). When statistically significant differences were observed, Tukey's mean comparison test was applied, with a significance level of 5%. The statistical analysis was performed using statistical software, ensuring a robust approach in interpreting the results.

3 RESULTS AND DISCUSSION

Table 2 shows that the films CPZ-P40, CP-P40, CPZ-P50, CP-A40, and CPZ-A50 differ significantly in terms of thickness increase when compared to the CP film (control). Despite being designed with pre-established values to achieve similar thicknesses, significant differences ($p < .05$) were observed among the formulations, which can be justified by the increase in solids content and the presence of fibers introduced into the film matrix (Adilah et al., 2018).

The moisture values ranged from 10.3 (CP Control) to 20.0% (CP-A40). All treatments showed higher moisture content than that found for the control (10.3%), indicating that the addition of pajurá and abiu flours, zinc nanoparticles, and rice wax can increase the moisture of CMC and pectin films. As reported in a study by Dong et al. (2022), films composed of CMC, pectin, and zinc nanoparticles showed moisture content consistent with the CP-P40, CPZ-P50, and CPZ-A50 films in this study. Treatments CP-AC and CPZ-PC, with values of 18.6 and 18.1, respectively, had results contrary to those found by Oliveira Filho et al. (2020), who reported that the presence of carnauba wax reduced the moisture content of the films. Regarding the treatment CP-A40 with higher moisture content (20%), it is observed that the formulation has a higher concentration of glycerol (50%), which may have influenced the result, consistent with the study on the production of corn starch films in combination with sorbitol and glycerol by Hazrol et al. (2021), where they concluded that the moisture content increased significantly as the concentration of plasticizers increased. Glycerol, due to its hydrophilic nature, retains water in the film matrix (Cerqueira et al., 2012).

The results of this study revealed a notable decrease in the solubility of the CPZ-A50 film, which is composed of CMC, pectin, ZnO-NPs, and abiu flour, with a value of 32.5 ± 0.34. This reduction can be attributed to the incorporation of zinc nanoparticles, which impart the film with a characteristic of lower solubility. According to Babapour et al. (2021), this effect can be explained by the formation of stronger hydrogen bonds between the polysaccharide network and the nanoparticles. The addition of ZnO nanoparticles to the polymeric matrix reduces the available hydroxyl groups for water molecules, resulting in decreased hydrophilicity of the films. The data obtained are in line with similar findings reported by Kanmani and Rhim (2014), where the formation of CMC with ZnO resulted in more hydrophobic films.

Consistent results with the present study were also presented by Jebel and Almasi (2016), whose study demonstrated a significant reduction of approximately 22% in the total moisture absorption when adding 5% of ZnO to the films. For the authors, this reduction can be attributed to the ability of cellulose fibers to establish new bonds with the oxygen groups present in ZnO, resulting in a reinforced structure that limits the diffusion of water molecules in the material. Remarkably, it can be observed that the CP-P40 and CP-A40 films exhibited higher solubility compared to the CPZ-P40 and CPZ-A50 compositions, which contained the addition of ZnO-NPs.

It is important to note that, with the exception of the CPZ-A50 treatment, all other films showed higher solubility compared to the CP control film (36.2 ± 0.69). This increase in solubility may have been influenced by various factors, such as the specific proportions of the ingredients used and possible interactions between these components.

Analyzing Table 2 in this study, it is noteworthy that the composite film of CMC and pectin (control treatment) recorded one of the lowest WVP indices (13.85 $g*m^{-2}*s^{-1}*Pa^{-1}$). One explanation for this observation is the cohesive nature of the films, which often exhibit lower porosity and, consequently, lower WVP (Silva et al., 2018).

In the CP-AC and CPZ-PC treatments, the addition of pajurá and abiu flour associated with rice wax (10.48 and 12.16 $g*m^{-2}*s^{-1}*Pa^{-1}$, respectively) played a crucial role in reducing the WVP, indicating superior water barrier properties.

Table 2. Thickness, moisture, water solubility, and water vapor permeability of treatments CP, CPZ-PC, CP-AC, CPZ-P40, CPZ-P50, CP-A40, and CPZ-A50.

Films	Thickness (mm)	Moisture (%)	Water solubility (%)	Water vapor permeability ($g*m^{-1}*s^{-1}*Pa^{-1}$)
CP (Control)	0.17 ± 0.01^{b}	10.3 ± 1.41^{b}	36.2 ± 0.69^{bc}	13.85 ± 0.95^{b}
CP-P40	0.27 ± 0.05^{ad}	14.8 ± 0.70^{ab}	48.3 ± 0.50^{a}	27.32 ± 0.27^{a}
CPZ-P40	0.25 ± 0.02^{acd}	11.2 ± 0.52^{ab}	38.1 ± 0.80^{bc}	14.25 ± 0.48^{b}
CPZ-P50	0.28 ± 0.02^{a}	16.7 ± 8.97^{ab}	41.6 ± 6.61^{abc}	11.66 ± 0.69^{b}
CP-A40	0.29 ± 0.01^{a}	20.0 ± 1.79^{a}	46.0 ± 0.57^{ab}	17.36 ± 0.30^{ab}
CPZ-A50	0.29 ± 0.03^{a}	16.2 ± 0.52^{ab}	32.5 ± 0.34^{c}	22.54 ± 0.13^{ab}
CP-AC	0.21 ± 0.01^{bcd}	18.6 ± 0.35^{ab}	40.4 ± 0.77^{abc}	10.48 ± 0.70^{b}
CPZ-PC	0.19 ± 0.01^{ab}	18.1 ± 0.76^{ab}	40.6 ± 7.37^{abc}	12.16 ± 0.26^{b}

*Same letters in the same column do not differ according to ($p < .05$).

This effect can be attributed to the presence of wax, whose hydrophobic character contributes to the decrease in permeability and the intensification of the vapor barrier. Previous studies, such as Oliveira Filho et al. (2020), confirm this phenomenon, reporting a significant reduction in WVP with the incorporation of carnauba wax, especially at a concentration of 15%, due to its hydrophobic nature.

The composition and concentration of the film are recognized as factors that influence the behavior of WVP, mainly through intermolecular interactions between the matrix and the compounds present. These interactions can impact the tortuosity pathway of water molecules in the film, resulting in different WVP values. For example, the introduction of 0.2g of ZnO-NPs and 1g of pajurá flour in the CPZ-P50 film (11.66 $g*m^{-2}*s^{-1}*Pa^{-1}$) provided a more complex pathway for water vapor to pass through the film matrix. As a direct result, a reduction in permeability was observed (Dash et al., 2019; Rodsamran & Sothornvit, 2019).

The CPZ-A50 film (22.54 $g*m^{-2}*s^{-1}*Pa^{-1}$) exhibited increased permeability compared to the other treatments. This characteristic can be attributed to the significant presence of hydrophilic compounds, such as phenolic compounds, in the abiu flour. The polyphenols present in abiu have the ability to disrupt the ordered structure of the film, leading to the formation of voids in its internal channels, as mentioned in previous studies (Barreiros & Barreiros, 2011; Thivya et al., 2022). The CP-P40 treatment achieved the highest result with a vapor permeability rate (27.32 $g*m^{-2}*s^{-1}*Pa^{-1}$), which may have been affected by the mixture of ingredients, which may not have been homogeneously made, leading to a lack of uniformity in the distribution of components. Table 3 presents the values of tensile strength (TS) and percent elongation at break (EB) for the analyzed polymers.

The analyzed polymeric films exhibited notable variations in TS and percent EB, with these variations directly influenced by the specific type of polymer employed. TS ranged from 3.93 to 40.32 MPa, while EB ranged from 3.54 to 45.40%. It was observed that the CP film (control) showed the best result for TS, a fact attributed to the similar chemical structure of CMC and pectin, leading to strong interactions between the composites, resulting in the formation of a denser matrix. The increase in mechanical properties of the film may have been caused by the intermolecular interaction between the carboxyl group of CMC and the hydroxyl group of polysaccharide molecules (Akhtar et al., 2018; Yu et al., 2014).

Table 3. Mechanical properties of films: tensile strength and percent elongation at break.

Films	TS (Mpa)	EB (%)
CP (controle)	40.32 ± 5.85^{a}	5.38 ± 2.22^{d}
CP-P40	7.00 ± 2.35^{cd}	18.85 ± 6.0^{c}
CPZ-P40	19.79 ± 2.83^{b}	3.54 ± 1.12^{d}
CPZ-P50	20.28 ± 2.24^{c}	4.17 ± 111^{d}
CP-A40	4.67 ± 1.01^{cd}	27.65 ± 4.24^{b}
CPZ-A50	3.93 ± 1.14^{d}	45.40 ± 7.65^{a}

* Same letters in the same column do not differ according to $p < 0.05$. TS: tensile strength; EB: elongation at break.

The comparison between the CPZ-P40 and CPZ-P50 treatments revealed no significant differences ($p < .05$) in the TS and EB values (Table 3). Both treatments showed reductions in TS values compared to the control film, while the EB values did not present statistically significant differences. However, it is notable that the TS values were higher compared to the other treatments, indicating robustness and lower flexibility. The inclusion of pajurá flour and zinc nanoparticles in the solution revealed chemical affinity of the polymers with the film-forming solution. These results were superior to the properties of films developed based on fruit and vegetable waste flour (FVR) (Brito et al., 2019), both for TS and EB.

The CP-A40, CPZ-A50, and CP-AC films had the worst results in terms of TS (4.6, 3.93, and 6.01 MPa) and EB (27.65, 45.40, and 30.92%), respectively. This reduction is attributed to the inclusion of abiu flour, which may have increased the free space and mobility of the polymers. This trend is similar to the study by Ahmad et al. (2015). In another study, Sougandhi et al. (2023) examined multifunctional bionanocomposite films with CMC, pectin, zinc nanoparticles, and guava extract and concluded that the addition of the extract and zinc nanoparticles improved the results of TS (8.43 MPa) and EB (18.54%). In contrast, the present study demonstrated inferior performance.

The addition of rice wax decreased the TS and increased the elongation of the films (Table 3), similar to the results obtained by Kowalczyk and Baraniak (2014), where, regardless of the type of biopolymer used, the presence of wax significantly decreased the mechanical strength of the films. In the same study, it is observed that the result of the film developed with CMC and candelilla wax has values similar to those of the CPZ-PC film in the present study. In Figure 1, the results of FTIR and Thermogravimetric Analysis (TGA) of the polymeric films are presented.

In Figure 1, it is observed that the composite films exhibit the typical band diagram of CMC, whose functional groups are similar to those of pectin, resulting in an overlap of peaks, as also observed in the study by Sharifi and Pirsa (2021).

The broad bands between 3400 and 3100 cm^{-1} in all samples indicate the presence of hydroxyl (-OH) groups with intermolecular hydrogen bonding stretches, common characteristics in polysaccharides. This observation is corroborated by studies by Li, Lu, et al. (2021). In the range of 2800–3000 cm^-1 (Figure 1), the peaks were identified as attributed to C-H, O-H, and NH3. These stretches are predominantly associated with carbohydrates, carboxylic acids, free amino acids, and phenolics (Anjos et al., 2015; Thummajitsakul et al., 2020). It is noteworthy that the CPZ-PC, CP-AC, and CPZ-A50 treatments exhibited higher intensity in this region, suggesting a higher concentration of the mentioned components in these formulations.

The region near 1730 cm^{-1} corresponds to the number of esterified carboxyl groups. The pronounced absorption band at 1590 cm^{-1} was attributed to the asymmetric and symmetric stretching of the COO^{-} group (Manrique & Lajolo, 2002).

The absorption band at 1460 cm^{-1} can be attributed to the combination of CH2 bending vibration and COO^{-} group vibration. This same spectral region has also been associated with

the presence of flavonols and organic acids, as per the study by Ibrahim et al. (2018). Additionally, the absorption band at 1320 cm^{-1} is related to symmetric deformations of CH2 linked to carboxyl groups. The fingerprint region from 1500 to 800 cm^{-1} is rich in peaks originating from various stretching, bending, rocking, scissoring, and twisting modes. This region is, on one hand, rich in information, but on the other hand, difficult to analyze due to its complexity. This area provides important information about organic compounds such as sugars, alcohols, and organic acids present in the sample (Lucarini et al., 2020).

Regarding the CP control film, differences in band intensities are observed in the CP-AC, CPZ-PC, CPZ-A50, CP-P40, and CP-A40 films both in the ~3299–3014 bands and in the 1000–1200 peaks, suggesting a higher amount of absorbed energy. It is also observed that the presence signal of phenols can be found in the region 1680–900 cm^{-1} (Silva et al., 2014), corresponding to a higher intensity of the mentioned films.

The absorption peaks between 1010 and 1150 cm^{-1} indicate that the sample contains pyranose. The absorption at 920 cm^{-1} refers to the absorption of D-glucopyranosyl (Zhang et al., 2013), in this study, fixed at 1014, 1020, and 918 cm^{-1} for all treatments.

Thermogravimetric analyses of the evaluated film systems revealed three distinct stages that characterize the thermal behavior of these materials (Figure 1B). In the temperature range of 35–190 °C, an initial weight loss of approximately 14% was observed in all samples, except for the CPZ-P40 and CPZ-P50 films, which exhibited weight losses around 27%. The initial reduction may be related to the evaporation of water contained in the samples, indicating a significant variation in the moisture content. This observation can be attributed to the hygroscopic properties of the biopolymers and glycerol, which are sensitive to environmental conditions, or to possible volatile compounds present in the films (Bátori et al., 2017; Sharifi & Pirsa, 2021).

The second stage occurred between temperature ranges of 210 and 340 °C, with the CPZ-P40 and CPZ-P50 films showing a mass loss of 80%, while the other treatments recorded a mass loss of 70%. This temperature corresponds to the degradation process, indicated by the significant mass loss. According to Rogovina et al. (2011), the temperatures confirm the degradation of polysaccharides, consistent with the range of 210–260 °C. In another study, chitosan and CMC films showed a considerable weight reduction of approximately 76% in the temperature range of 200–380 °C, indicating the complete pyrolysis of cellulose and the release of volatile hydrocarbons due to the rapid thermal decomposition of cellulose chains (Bajpai et al., 2015).

The third stage corresponded to the mass loss associated with the decomposition process of the polymeric matrix (Abutalib & Rajeh, 2020). In this study, the maximum decomposition temperature occurred around 340 °C.

Regarding the incorporation of zinc nanoparticles, it is observed that films showing higher mass loss may have undergone modifications in the polymeric structure after the addition of ZnO NPs. This is aligned with the findings of Noshirvani, Ghanbarzadeh, Mokarram, Hashemi, and Coma (2017), who demonstrated a reduction in the thermal stability of the polymer with the addition of ZnO NPs, especially when the concentration of ZnO NPs increased from 0.5 to 2%. On the other hand, it was also reported that the incorporation of ZnO NPs into pure carrageenan films resulted in increased thermal stability of the film (Roy & Rhim, 2019). Consequently, based on the TGA analysis, it can be inferred that the examined films exhibit satisfactory thermal stability for applications in the food packaging industry.

Figure 2 illustrates the differential scanning calorimetry (DSC) curves of all prepared films, while Table 4 presents the melting temperature (Tm) and the residue amount of the films. The results reveal that films CP, CPZ-P40, and CPZ-P50 exhibit higher melting temperatures (Tm) compared to the

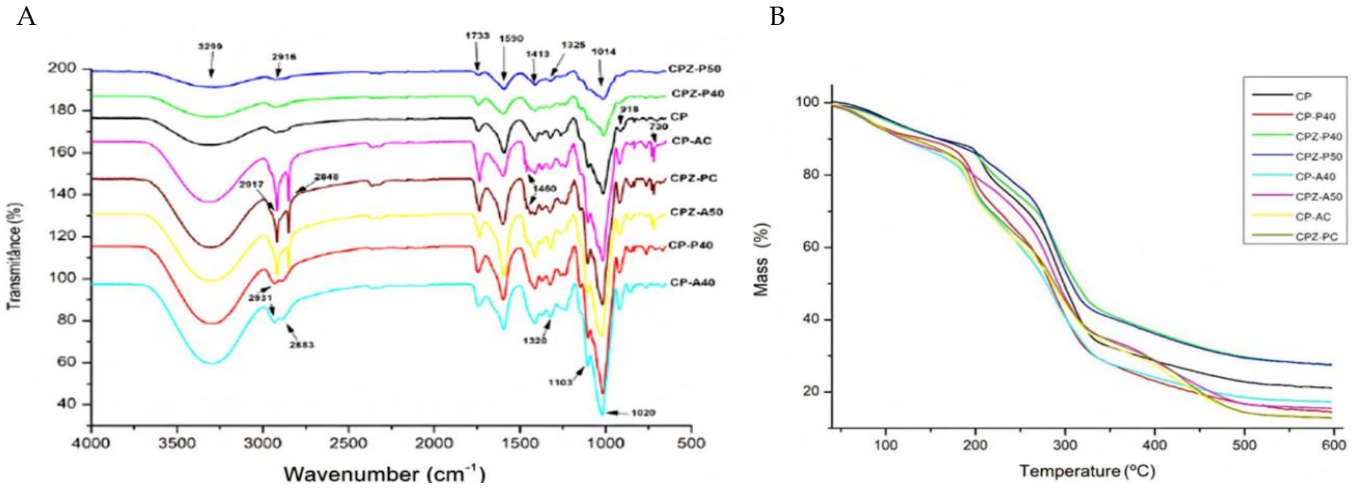

CP: carboxymethyl cellulose/pectin; CP-P40: carboxymethyl cellulose/pectin/glycerol/pajurá flour 40%; CPZ-P40: carboxymethyl cellulose/pectin/glycerol/zinc nanoparticles/pajurá flour 40%; CPZ-P50: carboxymethyl cellulose/pectin/glycerol/zinc nanoparticles/pajurá flour 50%; CP-A40: carboxymethyl cellulose/pectin/glycerol/abiu flour 40%; CPZ-A50: carboxymethyl cellulose/pectin/glycerol/zinc nanoparticles/abiu flour 50%; CP-AC: carboxymethyl cellulose/pectin/glycerol/abiu flour/rice wax; CPZ-PC: carboxymethyl cellulose/pectin/glycerol/zinc nanoparticles/pajurá flour/rice wax.

Figure 1. Absorption spectrum in the infrared region (Fourier Transform Infrared Spectra) (A) and thermogravimetric analysis (B) of films produced with carboxymethyl cellulose, pectin associated with pajurá flour, abiu flour, ZnO nanoparticles, and rice wax.

other treatments (except for film CP-P40, which showed only residual weight).

Additionally, the films exhibited only one endothermic peak, indicating the absence of phase separation, confirming the compatibility of the composite forming homogeneous films. These results are consistent with the phenomenon described by Charles et al. (2022), where films prepared with starch and potato peel starch also showed endothermic peaks and Tm above 100 °C. This suggests that the treatments did not undergo melting during the thermal treatment, demonstrating their potential use as a packaging material. Comparing the residual weight of the films, which ranged from 12.80 to 27.47% at 600 °C, depending on the type of filler, they showed a higher percentage of residues and, consequently, higher thermal stability.

The DSC analysis performed on films CP-A40, CPZ-A50, CP-AC, and CPZ-PC revealed the presence of multiple thermal transitions. Among these transitions, two endothermic varieties predominate, indicating heat absorption processes by the material. In the case of film CP-A40, an exothermic transition also occurs, characterized by heat release. In film CPZ-A50, two exothermic transitions are observed. The first endothermic peak may correspond to the evaporation of moisture and bound water from the films (Roy et al., 2021). It can be observed from the results that the composite films with added abiu flour and abiu flour/rice wax showed a significant decrease in peak area compared to the other treatments, indicating that the stability of the composite films was reduced. Subsequent decomposition occurred around 172–242 °C due to thermal degradation of the polymeric matrix of CMC, pectin, and glycerol used as a plasticizer (Li, Ren, et al., 2021; Priyadarshi et al., 2021; Roy & Rhim, 2019).

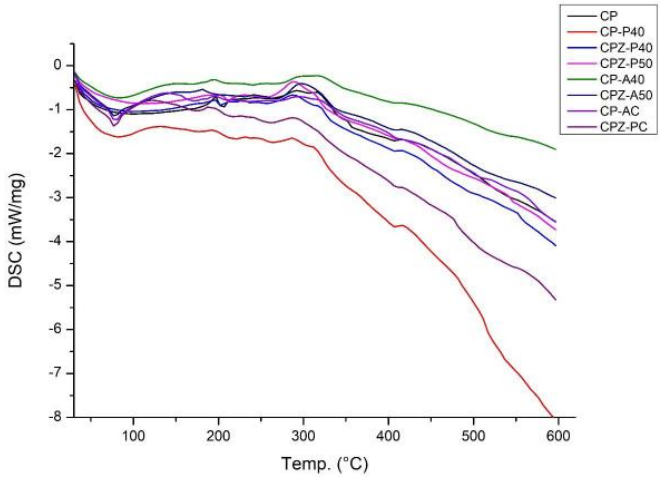

DSC: differential scanning calorimetry; CP: CMC/pectin; CP-P40: CMC/pectin/glycerol/pajurá flour 40%; CPZ-P40: CMC/pectin/glycerol/ZnO NPs/pajurá flour 40%; CPZ--P50: CMC/pectin/glycerol/ZnO NPs/pajurá flour 50%; CP-A40: CMC/pectin/glycerol/abiu flour 40%; CPZ-A50 (CMC/pectin/glycerol/ZnO/abiu flour); CP-AC: CMC/pectin/glycerol/abiu flour/rice wax; CPZ-PC: CMC/pectin/glycerol/ZnO/pajurá flour/rice wax.

Figure 2. Differential scanning calorimetry.

The results of thermal stability confirm the findings of the mechanical properties analysis. Treatments CP-A40 and CPZ-A50 exhibit distinct exothermic peaks at temperatures of 316.7 and 182.1 °C, respectively. These peaks can be attributed to the thermal degradation of the composite materials, especially due to the addition of abiu flour. This observation suggests that exothermic reactions occurred in the compounds during the heating process. These exothermic reactions may be related to thermal degradation processes, interactions between the components, or specific chemical reactions of the ingredients used.

The color evaluation of the tested films (Table 5) revealed notable modifications in chromatic properties after the incorporation of pajurá, abiu, and rice bran flours compared to the control film (CMC/pectin). Specifically, the CP-A40 film, containing abiu flour, stood out for showing lower luminosity (L*) values, indicating a darker hue, and elevated a* (hue between reddish and greenish) and b* (hue between yellowish and bluish) values.

Table 5. Effect of different treatments on Luminosity (L*), red-green axis color component (a*), and yellow-blue axis color component (b*).

Films	L*	a*	b*
CP	73.19 ± 7.40^{a}	2.61 ± 0.17^{c}	–0.59 ± 0.37^{e}
CP-P40	67.07 ± 0.84^{a}	2.70 ± 0.08^{c}	3.07 ± 0.11^{cd}
CPZ-P40	41.76 ± 7.44^{c}	4.34 ± 0.26^{b}	5.43 ± 0.29^{c}
CPZ-P50	40.00 ± 4.30^{c}	4.71 ± 0.34^{b}	4.40 ± 0.18^{c}
CP-A40	36.19 ± 4.24^{c}	5.43 ± 0.32^{a}	11.64 ± 0.63^{a}
CPZ-A50	47.75 ± 3.48^{bc}	5.62 ± 0.50^{a}	10.34 ± 0.87^{a}
CP-AC	64.48 ± 5.17^{ab}	3.77 ± 0.01^{bc}	8.70 ± 0.07^{b}
CPZ-PC	67.07 ± 2.01^{a}	3.33 ± 0.11^{c}	5.44 ± 0.34^{c}

Same letters in the same column do not differ according to ($p < .05$). L luminosity (0 = black – 100 = white), a* (–a* = green to +a* = red), and b* (–b* = blue to +b* = yellow).

Table 4. Thermal properties of the films: melting temperatures; exothermic peaks; and residual weight.

Films	Melting temperature (°C)	Melting temperature (°C)	Exothermic peaks (°C)	Exothermic peaks (°C)	Residual weight (%)
CP	203.7	-	-	-	20.22
CP-P40	-	-	-	-	14.89
CPZ-P40	202.4	-	-	-	27.28
CPZ-P50	209.1	-	-	-	27.47
CP-A40	83.5	242	316.7	-	17.26
CPZ-A50	78.4	-	182.1	297.5	15.48
CP-AC	78.6	172.7	-	-	13.04
CPZ-PC	78.5	175.5	-	-	12.80

The significant influence of the coloration of pajurá and abiu flours on the hue of the films is notable. The abundance of dark brown pigments in pajurá flour and the yellow carotenoids present in abiu flour substantially contributed to the coloration of the films that used these ingredients. These natural pigments can act as beneficial antioxidants for health (Gutiérrez & Álvarez, 2016).

It is worth noting that films with darker coloration have particularly relevant applications for light-sensitive foods. Packaging materials with denser and darker hues have the property of blocking ultraviolet (UV) rays, providing additional protection against the photo-oxidation process. This additional barrier is essential for preserving the quality of food over time, ensuring the maintenance of color, flavor, texture, and nutritional value of the products.

3.1 Evaluation of biodegradability

A qualitative study of material degradation based on the burial time of samples in natural organic soil was conducted.

On days 6, 9, and 12, significant and visible modifications were observed, particularly noticeable in the CP-P40, CP-A40, CPZ-A50, CP-AC, and CPZ-PC samples. In a study, pectin films containing fruit powders (raspberry, blackberry, and blueberry) showed similar results, with signs of biodegradation in the films observed after 6 days, and more significant degradation changes visualized after 12 days (Romero et al., 2022). On the 15th day, residue presence was observed in the CP (control), CPZ-P40, and CPZ-P50 treatments. However, it is important to note that at this stage, these residues were already undergoing biodegradation, indicating a trend toward material decomposition associated with these treatments.

It is noteworthy that films with pajurá flour and ZnO exhibited stiffer structures, justifying the longer degradation time. Conversely, the higher resistance to degradation of the CP film, composed of CMC, pectin, and glycerol, suggests that the intermolecular interaction between the polymeric components may have influenced the reduction in its biodegradability.

The European Standard EN 13432 stipulates that packaging must achieve a biodegradation rate of at least 90% within 6 months to be considered biodegradable by biological action. Based on this criterion, it is valid to consider the developed films as biodegradable, as they demonstrated the ability for degradation according to parameters established by the standard.

4 CONCLUSIONS

The formulations incorporating NPsZnO showed a significant reduction in solubility, better results for water vapor barrier, and mechanical resistance. Regarding thermal properties, all films exhibited good thermal stability with high melting temperatures in the DSC result, demonstrating resilience, with maximum decomposition temperatures around 340 °C.

Rice wax improved the water vapor barrier properties of the films, as well as imparting solubility and biodegradability properties.

The incorporation of Amazonian fruit flours in films emerges as an attractive choice, especially when considering the production of dark-toned packaging, which confers substantial advantages, particularly regarding the protection of light-sensitive foods, promoting an effective extension of their shelf life.

The CPZ-P40 and CPZ-P50 films stand out as excellent options for edible films, showing notable properties in permeability, mechanical resistance, and thermal stability. These films have the potential for application in various foods, especially those requiring protection against moisture and light. Pajurá flour stands out as a valuable component, showing potential to enhance film properties, which deserves attention in future research and practical applications.

ACKNOWLEDGMENTS

The authors express their sincere gratitude to the IF Goiano, FINEP, CAPES, and FAPEG for the financial support and infrastructure provided for the development of this work.

REFERENCES

Abreu, M. M. (2018). *Avaliação da atividade antidiarreica em camundongos e antimicrobiana in vitro do extrato bruto das cascas do fruto de Pouteria caimito (Ruiz e Pavon) Radlk* [Master's dissertation, Universidade Federal do Amapá]. Repositório UNIFAP. https://repositorio.unifap.br/bitstreams/0aa3327b-b8e0-487b-a53f-03d38f086b56/download

Abutalib, M. M., & Rajeh, A. (2020). Structural, thermal, optical and conductivity studies of Co/ZnO nanoparticles doped CMC polymer for solid state battery applications. *Polymer Testing*, *91*, Article 106803. https://doi.org/10.1016/j.polymertesting.2020.106803

Adilah, Z. A. M., Jamilah, B., & Hanani, Z. A. N. (2018). Functional and antioxidant properties of protein-based films incorporated with mango kernel extract for active packaging. *Food Hydrocolloids*, *74*, 207–218. https://doi.org/10.1016/j.foodhyd.2017.08.017

Ahmad, M., Hani, N. M., Nirmal, N. P., Fazial, F. F., Mohtar, N. F., & Romli, S. R. (2015). Optical and thermo-mechanical properties of composite films based on fish gelatin/rice flour fabricated by casting technique. *Progress in Organic Coatings*, *84*, 115–127. https://doi.org/10.1016/j.porgcoat.2015.02.016

Akhtar, H. M. S., Riaz, A., Hamed, Y. S., Abdin, M., Chen, G., Wan, P., & Zeng, X. (2018). Production and characterization of CMC-based antioxidant and antimicrobial films enriched with chickpea hull polysaccharides. *International Journal of Biological Macromolecules*, *118*, 469–477. https://doi.org/10.1016/j.ijbiomac.2018.06.090

American Society for Testing and Materials. (2009). *ASTM G160-03: Standard practice for evaluating microbial susceptibility of nonmetallic materials by laboratory soil burial* (Reapproved 2009). ASTM. https://doi.org/10.1520/G0160-03R09

Andrade, R. M. S. (2014). *Desenvolvimento e caracterização de filmes biodegradáveis à base de resíduos de frutas e hortaliças* [Master's dissertation, Universidade, Federal do Rio de Janeiro. Rio de Janeiro]. Repositório UNIRIO. https://www.unirio.br/proplan/ccbs/nutricao/ppgan_pt/dissertacoes-e-teses/dissertacoes-e-teses-defendidas/2011-2019/2014/desenvolvimento-e-caracterizacao-de-filmes-biodegradaveis-a-base-de-residuos-de-frutas-e-hortalicas

Anjos, O., Campos, M. G., Ruiz, P. C., & Antunes, P. (2015). Application of FTIR-ATR spectroscopy to the quantification of sugar in

honey. *Food Chemistry*, *169*, 218–223. https://doi.org/10.1016/j.foodchem.2014.07.138

Araújo, N. M. P., Arruda, H. S., Marques, D. R. P., Oliveira, W. Q., Pereira, G. A., & Pastore, G. M. (2021). Functional and nutritional properties of selected Amazon fruits: A review. *Food Research International*, *147*, Article 110520. https://doi.org/10.1016/j.foodres.2021.110520

Association of Official Analytical Chemists International. (2005). *Official Methods of Analysis of AOAC International* (18th ed.). AOAC International.

Babapour, H., Jalali, H., & Nafchi, M. A. (2021). The synergistic effects of zinc oxide nanoparticles and fennel essential oil on physicochemical, mechanical, and antibacterial properties of potato starch films. *Food Science & Nutrition*, *9*(7), 3893–3905. https://doi.org/10.1002/fsn3.2371

Bajpai, S. K., Chand, N., & Ahuja, S. (2015). Investigation of curcumin release from chitosan/cellulose micro crystals (CMC) antimicrobial films. *International Journal of Biological Macromolecules*, *79*, 440–448. https://doi.org/10.1016/j.ijbiomac.2015.05.012

Barreiros, A. L. B. S., & Barreiros, M. L. (2011, May 29–June 1). *Antioxidant activity of Amazonian fruits abiu (Pouteria caimito), biribá (Rollinia mucosa), and cubiu (Solanum sessiliflorum) by the DPPH scavenging method* [Paper presentation]. Anais da 34ª Reunião Anual da Sociedade Brasileira de Química. Aracaju, SE, Brazil.

Bátori, V., Jabbari, M., Åkesson, D., Lennartsson, P. R., Taherzadeh, M. J., & Zamani, A. (2017). Production of Pectin-Cellulose Biofilms: a new approach for citrus waste recycling. *International Journal of Polymer Science*, *2017*, Article 9732329. https://doi.org/10.1155/2017/9732329

Berto, A., Ribeiro, A. B., Sentandreu, E., Souza, N. E., Mercadante, A. Z., Chisté, R. C., & Fernandes, E. (2015). The seed of the Amazonian fruit Couepia bracteosa exhibits higher scavenging capacity against ROS and RNS than its shell and pulp extracts. *Food & Function*, *6*(9), 3081–3090. https://doi.org/10.1039/C5FO00722D

Brito, T. B., Carrajola, J. F., Gonçalves, E. C. B. A., Martelli-Tosi, M., & Ferreira, M. S. L. (2019). Fruit and vegetable residues flours with different granulometry range as raw material for pectin-enriched biodegradable film preparation. *Food Research International*, *121*, 412–421. https://doi.org/10.1016/j.foodres.2019.03.058

Cerqueira, M. A., Souza, B. W. S., Teixeira, J. A., & Vicente, A. A. (2012). Effect of glycerol and corn oil on physicochemical properties of polysaccharide films – A comparative study. *Food Hydrocolloids*, *27*(1), 175–184. https://doi.org/10.1016/j.foodhyd.2011.07.007

Charles, A. L., Motsa, N., & Abdillah, A. A. (2022). A comprehensive characterization of biodegradable edible films based on potato peel starch plasticized with glycerol. *Polymers*, *14*(17), Article 3462. https://doi.org/10.3390/polym14173462

Chiumarelli, M., & Hubinger, M. D. (2012). Stability, solubility, mechanical and barrier properties of cassava starch–Carnauba wax edible coatings to preserve fresh-cut apples. *Food Hydrocolloids*, *28*(1), 59–67. https://doi.org/10.1016/j.foodhyd.2011.12.006

Dash, K. K., Ali, N. A., Das, D., & Mohanta, D. (2019). Thorough evaluation of sweet potato starch and lemon-waste pectin based-edible films with nano-titania inclusions for food packaging applications. *International Journal of Biological Macromolecules*, *139*, 449–458. https://doi.org/10.1016/j.ijbiomac.2019.07.193

Dashipour, A., Razavilar, V., Hosseini, H., Shojaee-Aliabadi, S., German, J. B., Ghanati, K., Khakpour, M., & Khaksar, R. (2015). Antioxidant and antimicrobial carboxymethyl cellulose films containing Zataria multiflora essential oil. *International Journal of Biological Macromolecules*, *72*, 606–613. https://doi.org/10.1016/j.ijbiomac.2014.09.006

Dong, Z., Du, Z., Wu, X., Zhai, K., Wei, Z., & Rashed, M. M. A. (2022). Fabrication and characterization of ZnO nanofilms using extracted pectin of Premna microphylla Turcz leaves and carboxymethyl cellulose. *International Journal of Biological Macromolecules*, *209*(Part A), 525–532. https://doi.org/10.1016/j.ijbiomac.2022.04.030

Emamhadi, M. A., Sarafraz, M., Akbari, M., Thai, V. N., Fakhri, Y., Linh, N. T. T., & Khaneghah, A. M. (2020). Nanomaterials for food packaging applications: A systematic review. *Food and Chemical Toxicology*, *146*, Article 111825. https://doi.org/10.1016/j.fct.2020.111825

Espitia, P. J. P. (2013). *Desenvolvimento e avaliação de embalagens ativas antimicrobianas a base de metil celulose e polpa de açaí* [Doctoral dissertation, Universidade Federal de Viçosa]. Locus Repositório da UFV. https://locus.ufv.br/items/231eec9d-4b1d-4279-aa79-3a50ba95e798

Ezati, P., Riahi, Z., & Rhim, J.-W. (2022). CMC-based functional film incorporated with copper-doped TiO_2 to prevent banana browning. *Food Hydrocolloids*, *122*, Article 107104. https://doi.org/10.1016/j.foodhyd.2021.107104

Gan, L., Jiang, G., Yang, Y., Zheng, B., Zhang, S., Li, X., Tian, Y., & Peng, B. (2022). Development and characterization of levan/pullulan/chitosan edible films enriched with ε-polylysine for active food packaging. *Food Chemistry*, *388*, Article 132989. https://doi.org/10.1016/j.foodchem.2022.132989

Gutiérrez, T. J., & Álvarez, K. (2016). Physico-chemical properties and in vitro digestibility of edible films made from plantain flour with added Aloe vera gel. *Journal of Functional Foods*, *26*, 750–762. https://doi.org/10.1016/j.jff.2016.08.054

Hazrol, M. D., Sapuan, S. M., Zainudin, E. S., Zuhri, M. Y. M., & Wahab, N. I. A. (2021). Corn Starch (Zea mays) Biopolymer Plastic Reaction in Combination with Sorbitol and Glycero. *Polymers*, *13*(2), Article 242. https://doi.org/10.3390/polym13020242

Ibrahim, N., Zakaria, A. J., Ismail, Z., Ahmad, Y., & Mohd, K. S. (2018). Application of GCMS and FTIR Fingerprinting in discriminating two species of Malaysian stingless bees propolis. *International Journal of Engineering and Technology*, ResedarchGate, *7*(4.43), 106–112. http://eprints.unisza.edu.my/id/eprint/5809

Jebel, F. S., & Almasi, H. (2016). Morphological, physical, antimicrobial and release properties of ZnO nanoparticles-loaded bacterial cellulose films. *Carbohydrate Polymers*, *149*, 8–19. https://doi.org/10.1016/j.carbpol.2016.04.089

Jesus, L. S. (2017). *Produção de biofilmes á partir do mesocarpo externo do pequi (Caryocar brasilense Camb* [Master's dissertation Instituto Federal Goiano]. Repositório IF Goiano. https://repositorio.ifgoiano.edu.br/handle/prefix/29

Kanmani, P., & Rhim, J.-W. (2014). Properties and characterization of bionanocomposite films prepared with various biopolymers and ZnO nanoparticles. *Carbohydrate Polymers*, *106*, 190–199. https://doi.org/10.1016/j.carbpol.2014.02.007

Kouhi, M., Prabhakaran, M. P., & Ramakrishna, S. (2020). Edible polymers: an insight into its application in food, biomedicine and cosmetics. *Trends in Food Science & Technology*, *103*, 248–263. https://doi.org/10.1016/j.tifs.2020.05.025

Kowalczyk, D., & Baraniak, B. (2014). Effect of candelilla wax on functional properties of biopolymer emulsion films – a comparative study. *Food Hydrocolloids*, *41*, 195–209. https://doi.org/10.1016/j.foodhyd.2014.04.004

Li, X., Ren, Z., Wang, R., Liu, L., Zhang, J., Ma, F., Khan, M. Z. H., Zhao, D., & Liu, X. (2021). Characterization and antibacterial activity of edible films based on carboxymethyl cellulose, Dioscorea opposita mucilage, glycerol and ZnO nanoparticles. *Food Chemistry*, *349*, Article 129208. https://doi.org/10.1016/j.foodchem.2021.129208

Li, Y., Lu, J., Tian, X., Xu, Z., Huang, L., Xiao, H., Ren, X., & Kong, Q. (2021b). Alginate with citrus pectin and pterostilbene as healthy food packaging with antioxidant property. *International Journal of Biological Macromolecules*, *193*(Part B), 2093–2102. https://doi.org/10.1016/j.ijbiomac.2021.11.041

López, O. V., Lecot, C. J., Zaritzky, N. E., & García, M. A. (2011). Biodegradable packages development from starch based heat sealable films. *Journal of Food Engineering*, *105*(2), 254–263. https://doi.org/10.1016/j.jfoodeng.2011.02.029

Lucarini, M., Durazzo, A., Kiefer, J., Santini, A., Lombardi-Boccia, G., Souto, E. B., Romani, A., Lampe, A., Nicoli, S. F., Gabrielli, P., Bevilacqua, N., Campo, M., Morassut, M., & Cecchini, F. (2020). Grape seeds: chromatographic profile of fatty acids and phenolic compounds and qualitative analysis by FTIR-ATR spectroscopy. *Foods*, *9*(1), Article 10. https://doi.org/10.3390/foods9010010

Manrique, G. D., & Lajolo, F. M. (2002). FT-IR spectroscopy as a tool for measuring degree of methyl esterification in pectins isolated from ripening papaya fruit. *Postharvest Biology and Technology*, *25*(1), 99–107. https://doi.org/10.1016/S0925-5214(01)00160-0

Martelli, M. R., Barros, T. T., Moura, M. R., Mattoso, L. H. C., & Assis, O. B. G. (2013). Effect of chitosan nanoparticles and pectin content on mechanical properties and water vapor permeability of banana puree films. *Journal of Food Science*, *78*(1), N98–N104. https://doi.org/10.1111/j.1750-3841.2012.03006.x

Munhoz, C. L., Sanjinez-Argandoña, E. J., & Soares-Júnior, M. S. (2010). Extração de pectina de goiaba desidratada. *Food and Science Technology*, *30*(1), 119–125. https://doi.org/10.1590/S0101-20612010005000013

Nisar, T., Wang, Z.-C., Yang, X., Tian, Y., Iqbal, M., & Guo, Y. (2018). Characterization of citrus pectin films integrated with clove bud essential oil: Physical, thermal, barrier, antioxidant and antibacterial properties. *International Journal of Biological Macromolecules*, *106*, 670–680. https://doi.org/10.1016/j.ijbiomac.2017.08.068

Noshirvani, N., Ghanbarzadeh, B., Mokarram, R. R., Hashemi, M., & Coma, V. (2017). Preparation and characterization of active emulsified films based on chitosan-carboxymethyl cellulose containing zinc oxide nano particles. *International Journal of Biological Macromolecules*, *99*, 530–538. https://doi.org/10.1016/j.ijbiomac.2017.03.007

Oliveira Filho, J. G., Bezerra, C. C. O. N., Albiero, B. R., Oldoni, F. C. A., Miranda, M., Egea, M. B., Azeredo, H. M. C., & Ferreira, M. D. (2020). New approach in the development of edible fi;ms: The use of carnauba wax micro-or nanoemulsions in arrowroot starch-based films. *Food Packaging and Shelf Life*, *26*, Article 100589. https://doi.org/10.1016/j.fpsl.2020.100589

Pirouzifard, M., Yorghanlu, R. A., & Pirsa, S. (2019). Production of active film based on potato starch containing Zedo gum and essential oil of Salvia officinalis and study of physical, mechanical, and antioxidant properties. *Journal of Thermoplastic Composite Materials*, *33*(7), 915–937. https://doi.org/10.1177/0892705718815541

Priyadarshi, R., Kim, S.-M., & Rhim, J.-W. (2021). Pectin/pullulan blend films for food packaging: Effect of blending ratio. *Food Chemistry*, *347*, Article 129022. https://doi.org/10.1016/j.foodchem.2021.129022

Rodrigues, D. C., Caceres, C. A., Ribeiro, H. L., Abreu, R. F. A., Cunha, A. P., & Azeredo, H. M. C. (2014). Influence of cassava starch and carnauba wax on physical properties of cashew tree gum-based films. *Food Hydrocolloids*, *38*, 147–151. https://doi.org/10.1016/j.foodhyd.2013.12.010

Rodsamran, P., & Sothornvit, R. (2019). Lime peel pectin integrated with coconut water and lime peel extract as a new bioactive film sachet to retard soybean oil oxidation. *Food Hydrocolloids*, *97*(4), Article 105173. https://doi.org/10.1016/j.foodhyd.2019.105173

Rogovina, S. Z., Grachev, A. V., Aleksanyan, K. V., & Prut, E. V. (2011). Study of the thermal stability of blends based on synthetic polymers and natural polysaccharides. *Russian Journal of Bioorganic Chemistry*, *37*, 791–795. https://doi.org/10.1134/S1068162011070211

Romero, J., Cruz, R. M. S., Díez-Méndez, A., & Albertos, I. (2022). Valorization of berries' agro-industrial waste in the development of biodegradable pectin-based films for fresh salmon (Salmo salar) shelf-life monitoring. *International Journal of Molecular Sciences*, *23*(16), Article 8970. https://doi.org/10.3390/ijms23168970

Roy, S., Kim, H.-J., & Rhim, J.-W. (2021). Effect of blended colorants of anthocyanin and shikonin on carboxymethyl cellulose/agar-based smart packaging film. *International Journal of Biological Macromolecules*, *183*, 305–315. https://doi.org/10.1016/j.ijbiomac.2021.04.162

Roy, S., & Rhim, J.-W. (2019). Carrageenan-based antimicrobial bionanocomposite films incorporated with ZnO nanoparticles stabilized by melanin. *Food Hydrocolloids*, *90*, 500–507. https://doi.org/10.1016/j.foodhyd.2018.12.056

Sathiya, S. M., Okram, G. S., Dhivya, S. M., Mugesh, S., Murugan, M., & Rajan, M. A. J. (2018). Synergistic bactericidal effect of chitosan/zinc oxide based nanocomposites against Staphylococcus aureus. *Advanced Science Letters*, *24*(8), 5537–5542. https://doi.org/10.1166/asl.2018.12144.

Sharifi, K. A., & Pirsa, S. (2021). Biodegradable film of black mulberry pulp pectin/chlorophyll of black mulberry leaf encapsulated with carboxymethylcellulose/silica nanoparticles: Investigation of physicochemical and antimicrobial properties. *Materials Chemistry and Physics*, *267*, Article 124580. http://dx.doi.org/10.1016/j.matchemphys.2021.124580

Shivangi, S., Dorairaj, D., Negi, P. S., & Shetty, N. P. (2021). Development and characterisation of a pectin-based edible film that contains mulberry leaf extract and its bio-active components. *Food Hydrocolloids*, *121*, Article 107046. https://doi.org/10.1016/j.foodhyd.2021.107046

Silva, C. A. M., Simeoni, L. A., & Silveira, D. (2009). Genus Pouteria: chemistry and biological activity. *Revista Brasileira de Farmacognosia*, *19*(2a), 501–509. https://doi.org/10.1590/S0102-695X2009000300025

Silva, K. S., Fonseca, T. M. R., Amado, L. R., & Mauro, M. A. (2018). Physicochemical and microstructural properties of whey protein isolate-based films with addition of pectin. *Food Packaging and Shelf Life*, *16*, 122–128. https://doi.org/10.1016/j.fpsl.2018.03.005

Silva, M. A., Bierhalz, A. C. K., & Kieckbusch, T. G. (2009). Alginate and pectin composite films crosslinked with Ca2+ ions: Effect of the plasticizer concentration. *Carbohydrate Polymers*, *77*(4), 736–742. https://doi.org/10.1016/j.carbpol.2009.02.014

Silva, S. D., Feliciano, R. P., Boas, L. V., & Bronze, M. R. (2014). Application of FTIR-ATR to Moscatel dessert wines for prediction of total phenolic and flavonoid contents and antioxidant capacity. *Food Chemistry*, *150*, 489–493. https://doi.org/10.1016/j.foodchem.2013.11.028

Sougandhi, P. R., Jena, S. K., Brahmanand, P. S., Tej, M. B., Kadiyala, N. K., Rani, T. S., & Rao, M. V. B. (2023). Multifunctional bio-nanocomposite films of carboxymethyl cellulose and pectin

with incorporated zinc oxide nanoparticles. *Letters in Applied NanoBioScience*, *12*(3), Article 85. https://doi.org/10.33263/LIANBS123.085

Thivya, P., Bhosale, Y. K., Anandakumar, S., Hema, V., & Sinija, V. R. (2022). Study on the characteristics of gluten/alginate-cellulose/onion waste extracts composite film and its food packaging application. *Food Chemistry*, *390*, Article 133221. https://doi.org/10.1016/j.foodchem.2022.133221

Thummajitsakul, S., Samaikam, S., Tacha, S., & Silprasit, K. (2020). Study on FTIR spectroscopy, total phenolic content, antioxidant activity and anti-amylase activity of extracts and different tea forms of Garcinia schomburgkiana leaves. *LWT*, *134*(1), Article 110005. https://doi.org/10.1016/j.lwt.2020.110005

Turbiani, F. R. B., & Kieckbusch, T. G. (2011). Propriedades mecânicas e de barreira de filmes de alginato de sódio reticulados com benzoato de cálcio e/ou cloreto de cálcio. Brazilian *Journal of Food Technology*, *14*(2), 82–90. https://doi.org/10.4260/BJFT2011140200011

Yu, W.-X., Wang, Z.-W., Hu, C.-Y., & Wang, L. (2014). Properties of low methoxyl pectin-carboxymethyl cellulose based on montmorillonite nanocomposite films. *International Journal of Food Science & Technology*, *49*(12), 2592–2601. https://doi.org/10.1111/ijfs.12590

Zhang, L., Ye, X., Ding, T., Sun, X., Xu, Y., & Liu, D. (2013). Ultrasound effects on the degradation kinetics, structure and rheological properties of apple pectin. *Ultrasonics Sonochemistry*, *20*(1), 222–231. https://doi.org/10.1016/j.ultsonch.2012.07.021